ISSN 1063-7826, Semiconductors, 2018, Vol. 52, No. 5, pp. 675–677. © Pleiades Publishing, Ltd., 2018.

XXV INTERNATIONAL SYMPOSIUM
"NANOSTRUCTURES: PHYSICS AND TECHNOLOGY",
SAINT PETERSBURG, RUSSIA, JUNE 26–30, 2017.
NANOSTRUCTURE TECHNOLOGY

Dip-Pen Nanolithography Method for Fabrication of Biofunctionalized Magnetic Nanodiscs Applied in Medicine[1]

T. E. Smolyarova[a, b]*, A. V. Lukyanenko[a, b], A. S. Tarasov[a, b], and A. E. Sokolov[a, b]

[a] *Siberian Federal University, Krasnoyarsk, 660041 Russia*

[b] *Kirensky Institute of Physics, Russian Academy of Science, Krasnoyarsk, 660036 Russia*

**e-mail: smol_nano@iph.krasn.ru*

Received December 25, 2017

Abstract—The magnetic properties of ferromagnetic nanodiscs coated with gold, manufactured using the Dip-Pen Nanolithography method, and were studied by atomic-force and magnetic force microscopy methods. The magnetic discs (dots) are represented as nanoagents (nanorobots) applied in medicine for the cancer cell destruction. The motivation of this work stem from the necessity of the understanding of the magnetization distribution in ferromagnetic discs that is crucial for their application in biomedicine. We have performed the theoretical calculations in order to compare the theoretical image contrast to experimental results. Herein, we report about the fabrication and analysis of biocompatible ferromagnetic nanodiscs with the homogenous magnetized state.

DOI: 10.1134/S1063782618050305

1. INTRODUCTION

Nowadays magnetic nanoparticles have a great potential to be applied in biomedical fields such as magnetic resonance imaging (MRI) [1–3], magnetic separation [4–6], magnetic hyperthermia therapy [7, 8], and drug delivery [9, 10].Magnetic hyperthermia is the most famous method for the local therapy of the tumor. A wide variety of shapes and sizes of the particles allows them to interact with biological objects: viruses, ribonucleic acid, proteins, cells and organelles [11]. Magnetic nanoparticles can be used in the form of powders or suspensions, but very often different coatings are used for their introduction into a biological object to perform several functions at once: reduce the toxicity of nanoparticles and preventtheir degradation in the body [12]. We fabricated the magnetic nanodiscs are able to destroy cancer cells. The structure of the nanodiscs is multilayered and consists of ferromagnetic FeNi covered with Au. When an alternating magnetic field is applied the nanodisc vortex core shifts, creating an oscillation, which transmits a mechanical force to the cell. Then this mechanical force is efficiently transduced to the membrane and further on to subcellular components [13, 14]. Besides this ferromagnetic nanodiscs can also be used in hyperthermia method. Currently, photolithography, electron beam lithography and nanoimprint lithography are used to fabricate magnetic nanodiscs [15–17]. We demonstrate a new approach to fabricate biocompatible ferromagnetic nanodiscs using Dip-Pen Nanolithography (DPN) method on the Au/NiFe/Au/Al/Si(111) structure. Atomic Force Microscope NanoInk, Inc. DPN 5000 includes three operation modes: atomic force microscopy (AFM) was applied to scan the topographic features of the film, magnetic force microscopy (MFM) was used to image the magnetic forces and system of Dip-Pen Nanolithography was used to create nanostructured array of ferromagnetic nanodiscs.

2. EXPERIMENTAL

In DPN, the tip of an atomic force microscope probe is coated with ink and traced across a target surface. As the probe traverses the surface, the ink is deposited along the tracing path and diffuses away from the tip through the water meniscus. By varying the tip speed and/or dwell time, it is possible to create lines of various widths and/or dots of various radii, and the lines and dots can be combined to create complex patterns. The instrument uses an environmental chamber capable of controlling temperature and relative humidity through a real-time feedback loop. Environmental conditions were kept constant throughout all experiments. The NanoInk Chamber software permits environmental stabilization while being able to avoid associated noise by turning off the heater and nebulizer during writing and imaging.

[1]The article is published in the original.

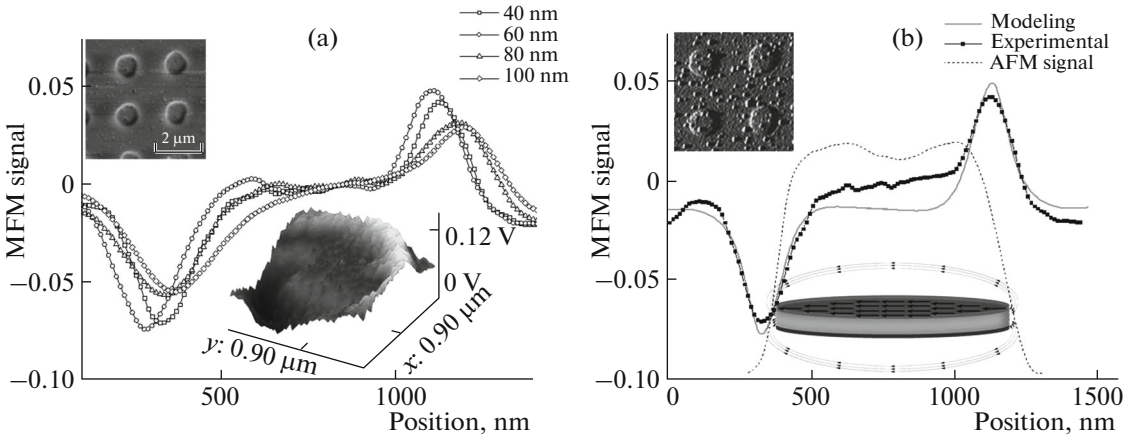

Fig. 1. (a) the cross-section of MFM signals of the same disc in different lift heights, 3D representation of the magnetization distribution and image of MFM signal of Au/NiFe/Au discs; (b) model calculation of magnetic force signal (grey line) and the measured MFM signal (black-squared line) on the lift-height of 40 nm compared with the AFM signal (dotted line) and topological signal image of Au/NiFe/Au discs.

As mentioned, previous DPN work varied environmental conditions while keeping the tip and structure the same. While exploring minimum line width dependencies on surface roughness and tip radius, we kept environmental conditions stable at $T = 27 \pm 0.1$°C and RH = 38 ± 0.5%. This way we formed the nanostructured array of nanodiscs on the Au/NiFe/Au/Al/Si(111) structure using the SiN probe coated with MHA-Acetonitrile. We use the Al film for the last stage of nanodiscs fabrication. The chemical etching of this layer allows to lift off the nanodiscs from the substrate.

After DPN procedure structure patterned with the polymer (MHA-Acetonitrile) was operated by four-stage chemical etching process. Firstly, the structure was treated for 20 minutes in the wet etching of 1:1:1:1 (v/v/v/v) aqueous mixture of 0.1 M $Na_2S_2O_3$, 1.0 M KOH, 0.01 M $K_3Fe(CN)_6$ and 0.001 M $K_4Fe(CN)_6$ [18] with constant stirring to completely remove Au from areas aren't covered with MHA-polymer. Secondly, the sample was treated in dilute solution of HNO_3 for 1 minute with constant heating to completely remove NiFe film. Thirdly, the structure was treated again to remove the second Au film. Thus 30-nm-thick, 0.9-μm-diameter Au/NiFe/Au were fabricated by DPN method on the Si(111) structure. After cleaning in acetone ($CH_3 + C(O) + CH_3$) to remove the MHA polymer from the disc surface, water (H_2O) and drying with nitrogen (N_2), getting structure was analyzed in contact magnetic force mode (MFM) of AFM.

For the MFM investigations we employed a Nanoink Inc. DPN 5000 scanning probe microscope in noncontact mode and phase detection of the magnetic force gradients. Commercial MFM 40 nm tips coated with CoCr were used. The lift-height was set to 40, 60, 80 and 100 nm. All MFM measurements were carried out at ambient conditions. The MFM mode of SPM NanoInk, Inc. DPN 5000 was used to analyze magnetic signal. This mode is operated together with AFM. Atomic force is a short-range force while magnetic force is a long ranged one. By lifting the MFM tip away from the medium from the topographic scanning (AFM) to the magnetic scanning (MFM), the major portion of the atomic force will be eliminated in the MFM signal.

When conducting magnetic studies at the submicron level, first of all, it is necessary to separate the MFM images from the topology images (AFM). To solve this problem, magnetic measurements are carried out using a two-pass method. On the first pass, the surface topology is determined by semi-contact methods. On the second pass of each scan line (or the image as a whole), the cantilever is raised above the surface and scanning is performed in accordance with the stored path. As a result, on the second pass, the distance between the scanned surface and the fixed end of the cantilever is kept constant. In accordance with this method, both the AFM image and the MFM image were obtained simultaneously. Fabricated nanostructured array of ferromagnetic nanodiscs was studied by MFM mode to display the magnetic signal on different lift heights: 40, 60, 80 and 100 nm (Fig. 1a).

The MFM probe used for the measurement was oriented perpendicular to the sample ($\alpha = 90°$) and the cantilever was tilted at an angle $\beta_c = 4°$ with respect to the sample plane. With this probe configuration, the magnetic transitions appear as either dark or bright spots, corresponding to attractive or repulsive force derivatives, respectively. This response is shown explicitly by the constant force derivative contour in Fig. 1a.

Experimental MFM image of fabricated 0.9-μm Au/NiFe/Au nanodiscs has the ground state of the homogenous magnetization, oriented along the direction of the external magnetic field (Fig. 1a). This image shows that all nanodiscs demonstrate the dipole distribution of MFM contrast typical for homogenous magnetized state.

The MFM signal of fabricated nanodiscs is dependent of the lift-height in MFM scanning: higher lift-height leads to lower magnetic signal. The distribution of the magnetic signal in the ferromagnetic nanodisc occurs according to the magnetic force lines of the disc. Thus, we observe two differently directed peaks in the cross-sections and in the 3D model of the MFM signal (Fig. 1a). According to the MFM research the size of the magnetic signal does not equal to the one-dimensional profile of the disc (Fig. 1b), so the actual diameter of fabricated nanodiscs is 0.9-μm. Thus, magnetic force lines most probably lie outside of the ferromagnetic disc and the vector of the magnetization lies inside of the disc. We support that the sizes of the disc align with the domain sizes.

A number of previous authors have calculated the forces resulting from various magnetizations of probe and sample [19–21]. We have performed the similar calculations order to compare the theoretical image contrast to the experimental results

The calculations of the magnetic force signal are calculated for a cantilever oriented at the angle $\beta_c = 4°$ and the probe perpendicular ($\alpha = 90°$) to the sample. The calculation predicts unipolar symmetric peaks, reflecting to the basic model described earlier in [22]. The good agreement between modeling and experiment in Fig. 1b supports the presumption that the tip magnetization is aligned predominantly perpendicular to the sample axis.

3. RESULTS

We demonstrated the new approach to fabricate biofunctionalized magnetic nanodiscs using the DPN method. Fabricated 30-nm-thick, 0.9-μm-diameter Au/NiFe/Au single-domain magnetic nanodiscs nontoxic and suitable for the targeted cancer-cell destruction due to its size and the ability to bind cells selectively when the magnetic field is applied.

The magnetic force microscopy method allows us the concept about the magnetization distribution and its orientation. To take the magnetic measurements of the nanodiscs the dynamic mode of the magnetic force microscopy method was used. Fabricated nanodiscs are multilayered single domain structures with the homogenous magnetized state. The shape and the type of the magnetic force contrast curve were obtained experimentally and compared with the theoretical model.

ACKNOWLEDGMENTS

The study was funded by Russian Foundation for Basic Research, Government of Krasnoyarsk Territory, Krasnoyarsk Region Science and Technology Support Fund to the research project nos. 17-42-240080, 16-42-243046, 16-42-242036 and the Grant of the President of the Russian Federation no. NSh-7559.2016.2.

REFERENCES

1. F. Q. Hu, L. Wei, Z. Zhou, Y. L. Ran, Z. Li, and M. Y. Gao, Adv. Mater. **18**, 2553 (2006).
2. J. Yu, C. Yang, J. Li, Y. Ding, L. Zhang, M. Z. Yousaf, J. Lin, R. Pang, L. Wei, L. Xu, F. Sheng, C. Li, G. Li, L. Zhao, and Y. Hou, Adv. Mater. **26**, 4114 (2014).
3. D. Liu, W. Wu, J. Ling, S. Wen, N. Gu, and X. Zhang, Adv. Funct. Mater. **21**, 1498 (2011).
4. S. Carinelli, M. Martı, S. Alegret, and M. I. Pividori, New Biotechnol. **32**, 521 (2015).
5. J. B. Haun, C. M. Castro, R. Wang, V. M. Peterson, B. S. Marinelli, H. Lee, and R. Weissleder, Sci. Transl. Med. **3** (71), ra16 (2011).
6. C. T. Yavuz, J. T. Mayo, W. Y. William, A. Prakash, J. C. Falkner, S. Yean, L. Cong, H. J. Shipley, A. Kan, M. Tomson, D. Natelson, and V. L. Colvin, Science **314**, 964 (2006).
7. R. Hergt, S. Dutz, R. Muller, and M. Zeisberger, J. Phys.: Condens. Matter **18**, 2919 (2006).
8. C. S. Kumar and F. Mohammad, Adv. Drug. Deliver. Rev. **63**, 789 (2011).
9. M. Arruebo, R. Fernandez-Pacheco, M. R. Ibarra, and J. Santamaria, Nano Today **2**, 22 (2007).
10. J. Dobson, Drug. Dev. Res. **67**, 55 (2006).
11. M. J. Li, A. Nath, and W. M. Atkins, Biochemistry **56**, 2506 (2017).
12. R. BrittoHurtado, M. Cortez-Valadez, and H. Arizpe-Chavez, Gold Bull. **50**, 85 (2017).
13. X. L. Liu and H. M. Fan, Curr. Opin. Chem. Eng. **4**, 38 (2014).
14. E. A. Rozhkova, I. V. Ulasov, S. D. Baderl, M. S. Lesniak, and D. H. Kim, Nat. Mater. **10**, 165 (1964).
15. V. Suresh, M. S. Huang, and M. P. Srinivasan, J. Mater. Chem. **22**, 21871 (2012).
16. M. Buerger, M. Ruth, S. Declair, J. Forstner, C. Meier, and D. J. As, Appl. Phys. Lett. **102**, 081105 (2013).
17. L. X. Zou, X. M. Lv, and Y. Z. Huang, Opt. Lett. **38**, 3807 (2013).
18. S. W. Chung, A. Mirkin, and H. Zhang, Nano Lett. **3**, 43 (2010).
19. J. J. Saenz, N. Garcia, P. Grutter, E. Meyer, H. Heinzelmann, R. Weisendanger, L Rosenthaler, H. R. Hidber, and H.-J. Guntherodt, J. Appl. Phys. **62**, 4293 (1987).
20. A. Wadas, J. Magn. Magn. Mater. **71**, 147 (1988).
21. I. I. Saenz, N. Garcia, and J. C. Slonczewski, Appl. Phys. Lett. **53**, 1449 (1988).
22. D. Rugar, H. J. Mamin, P. Guethner, S. E. Lambert, and J. E. Stern, J. Appl. Phys. **68**, 1169 (1990).